This is a preprint, the final version is subject to change, of the American Mineralogist (MSA)
Cite as Authors (Year) Title. American Mineralogist, in press.
(DOI will not work until issue is live.) DOI: http://dx.doi.org/10.2138/am-2016-5636

Revision 1

The crystal structure of svabite, $Ca_5(AsO_4)_3F$, an arsenate member of the apatite supergroup

CRISTIAN BIAGIONI[1*], FERDINANDO BOSI[2,3], ULF HÅLENIUS[4], and MARCO PASERO[1]

[1] *Dipartimento di Scienze della Terra, Università di Pisa, Via S. Maria 53, I-56126 Pisa, Italy*

[2] *Dipartimento di Scienze della Terra, Sapienza Università di Roma, Piazzale Aldo Moro 5, I-00185 Roma, Italy*

[3] *CNR – Istituto di Geoscienze e Georisorse, UOS Roma, Piazzale Aldo Moro 5, I-00185 Roma, Italy*

[4] *Department of Geosciences, Swedish Museum of Natural History, Box 50007, SE-10405 Stockholm, Sweden*

**e-mail address: biagioni@dst.unipi.it*

Always consult and cite the final, published document. See http:/www.minsocam.org or GeoscienceWorld

This is a preprint, the final version is subject to change, of the American Mineralogist (MSA)
Cite as Authors (Year) Title. American Mineralogist, in press.
(DOI will not work until issue is live.) DOI: http://dx.doi.org/10.2138/am-2016-5636

ABSTRACT

The crystal structure of svabite, ideally $Ca_5(AsO_4)_3F$, was studied using a specimen from the Jakobsberg mine, Värmland, Sweden, by means of single-crystal X-ray diffraction data. The structure was refined to $R_1 = 0.032$ on the basis of 928 unique reflections with $F_o > 4\sigma(F_o)$ in the $P6_3/m$ space group, with unit-cell parameters $a = 9.7268(5)$, $c = 6.9820(4)$ Å, $V = 572.07(5)$ Å^3. The chemical composition of the sample, determined by electron-microprobe analysis, is (in wt% - average of 12 spot analyses): SO_3 0.49, P_2O_5 0.21, V_2O_5 0.04, As_2O_5 51.21, SiO_2 0.19, CaO 39.31, MnO 0.48, SrO 0.03, PbO 5.19, Na_2O 0.13, F 2.12, Cl 0.08, H_2O_{calc} 0.33, O (≡ F+Cl) –0.91, total 98.90. On the basis of 13 anions per formula unit, the empirical formula corresponds to $(Ca_{4.66}Pb_{0.16}Mn_{0.04}Na_{0.03})_{\Sigma 4.89}(As_{2.96}S_{0.04}Si_{0.02}P_{0.02})_{\Sigma 3.04}O_{12}[F_{0.74}(OH)_{0.24}Cl_{0.01}]$. Svabite is topologically similar to the other members of the apatite supergroup: columns of face-sharing *M*1 polyhedra running along **c** are connected through TO_4 tetrahedra with channels hosting *M*2 cations and *X* anions. The crystal structure of synthetic $Ca_5(AsO_4)_3F$ was previously reported as triclinic. On the contrary, the present refinement of the crystal structure of svabite shows no deviations from the hexagonal symmetry. An accurate knowledge of the atomic arrangement of this apatite-remediation mineral represents an improvement in our understanding of minerals able to sequester and stabilize heavy metals such as arsenic in polluted areas.

Key-words: svabite, calcium arsenate, apatite supergroup, crystal structure, Jakobsberg mine, Sweden.

Always consult and cite the final, published document. See http:/www.minsocam.org or GeoscienceWorld

Introduction

The general formula of the members of the apatite supergroup is $^{IX}M1_2{}^{VII}M2_3(^{IV}TO_4)_3X$. Svabite is a rare member of the supergroup with $M1 = M2 = Ca$, $T = As$, $X = F$ and ideal formula $Ca_5(AsO_4)_3F$. Historically, svabite was described as the arsenate analogue of "apatite" (Sjögren 1891, 1892) at a time when little attention was paid to the nature of the *X* anion as a discriminant between distinct species. As a consequence, the original description of svabite was based on analyses of samples from two different localities (Harstigen mine, Persberg district, and Jakobsberg mine, Nordmark district) in the Långban mining area, Värmland, Sweden.

The analyses were different: the sample from Harstigen was fluorine-free, the sample from Jakobsberg had some 2 wt.% F. According to the current definition of mineral and to the specific guidelines for the nomenclature of apatite supergroup minerals (Pasero et al. 2010), the sample from Harstigen corresponds to johnbaumite, the sample from Jakobsberg to svabite. This notwithstanding, it is Harstigen that has been designated as the type locality for svabite (e.g., Palache et al. 1951; Gaines et al. 1997), although svabite probably does not occur there.

Since then, svabite was reported from very few other localities worldwide. In two cases only chemical analyses are given for the mineral: from Franklin, New Jersey, U.S.A. (Bauer and Berman 1930), and from the Solongo boron deposit, Buryatia, Siberia, Russia (Malinko et al. 1966). At both these localities, OH is dominant and therefore the alleged svabite is actually johnbaumite. As a consequence, the unique unequivocal occurrence of svabite is the Jakobsberg mine, based on a wet chemical analysis dating back to the 19th Century and to an electron-microprobe analysis given by Welin (1968). A crystal structure refinement of svabite was never carried out. The only available structural data are for synthetic $Ca_5(AsO_4)_3F$ (Baikie et al. 2007).

As understanding the atomic arrangements of As-rich apatite minerals would help to better refine their utility in environmental remediation (Rakovan and Pasteris 2015), we undertook a

Always consult and cite the final, published document. See http:/www.minsocam.org or GeoscienceWorld

chemical and crystallographic re-examination of material from the Jakobsberg mine, aiming to confirm the occurrence of svabite at the type locality, and to refine its crystal structure.

Experimental

The studied specimen consists of a fine- to medium-grained mixed hausmannite and jacobsite mineralization in which cm-sized areas of white to pale rose-colored assemblages of fine- to medium-grained svabite and tilasite occur. Associated accessory and minor mineral phases are baryte, dolomite, oxycalcioroméite, berzeliite, and adelite. This specimen was donated together with his large mineral collection by Hjalmar Sjögren to the Swedish Museum of Natural History in 1902. In the catalogue of this donation there exists two specimens from Jakobsberg labeled "svabite" that were recorded as chemically analysed. It seems very likely that the analyses of svabite from Jakobsberg reported by Sjögren in 1892 were obtained on these two samples. The presently studied svabite comes from one of these two specimens (Swedish Museum of Natural History catalogue #HS0255).

Electron microprobe analyses were obtained by wavelength dispersive spectroscopy (WDS mode) with a Cameca SX50 instrument at the "Istituto di Geologia Ambientale e Geoingegneria, CNR" of Rome, Italy, using the following analytical conditions: accelerating voltage 15 kV, beam current 15 nA, nominal beam diameter 1 μm. Counting time for one spot analysis was 20 s per peak. Standards (element, emission line) are: baryte (Ba*L*α, S*K*α), YPO_4 (P*K*α), GaAs (As*L*α), wollastonite (Ca*K*α, Si*K*α), vanadinite (V*K*α), rhodonite (Mn*K*α), celestine (Sr*K*α), galena (Pb*M*α), jadeite (Na*K*α), phlogopite (F*K*α), and sylvite (Cl*K*α). The PAP routine was applied (Pouchou and Pichoir 1991) for correction of recorded raw data. Twelve spot analyses were performed on five different grains that were found homogeneous. Chemical data are given in Table 1; the chemical formula, based on 13 anions per formula unit, is $(Ca_{4.66}Pb_{0.16}Mn_{0.04}Na_{0.03})_{\Sigma 4.89}(As_{2.96}S_{0.04}Si_{0.02}P_{0.02})_{\Sigma 3.04}O_{12}[F_{0.74}(OH)_{0.24}Cl_{0.01}]$.

Always consult and cite the final, published document. See http:/www.minsocam.org or GeoscienceWorld

Polarised single-crystal infrared spectra of svabite and johnbaumite (catalogue #19642 of the mineralogical collection of the Museo di Storia Naturale, University of Pisa) were recorded with a Bruker Vertex 70 microscope spectrometer equipped with a halogen lamp source, a KBr beam-splitter, a holographic ZnSe polarizer and a midband MCT detector. The crystals were oriented by morphology and optical microscopy and doubly polished parallel to the **a**-**c** axis plane. The thickness of the single crystal absorbers were in the range 17 to 46 μm. Polarized absorption spectra were acquired parallel (E||E) and perpendicular (E||O) to the **c**-axis over the wavenumber range 600–5000 cm^{-1} with a resolution of 2 cm^{-1} during 32 cycles. In addition, unpolarised spectra of powdered svabite (ca. 1 mg) in pressed KBr discs were recorded under identical conditions in order to monitor the very intense IR-active AsO_4-modes in the range 700–1000 cm^{-1}. The spectral region of the O–H stretching bands of the recorded single-crystal spectra were fitted using the *PeakFit* 4.12 software (Jandel) assuming Gaussian peak shapes.

A crystal fragment (230 × 80 × 50 μm^3 in size) was selected for single-crystal X-ray diffraction. Intensities were collected using a Bruker Smart Breeze diffractometer (50 kV, 30 mA) equipped with a CCD 4k low-noise area detector. Graphite-monochromatized Mo*K*α radiation was used. The detector-to-crystal working distance was 50 mm. 3035 frames were collected in ω and φ scan modes in 0.5° slices; the exposure time was 20 s per frame. The data were integrated and corrected for Lorentz and polarization, background effects, and absorption using the package of softwares *Apex*2 (Bruker AXS Inc. 2004), resulting in a set of 1008 independent reflections. The refinement of unit-cell parameters constrained to hexagonal symmetry gave a = 9.7268(5), c = 6.9820(4) Å, V = 572.07(5) $Å^3$. The statistical tests on the distribution of $|E|$ values ($|E^2 - 1|$ = 0.966) and the systematic absences suggested the space group $P6_3/m$.

The crystal structure was refined starting from the atomic coordinates of johnbaumite given by Biagioni and Pasero (2013) using *Shelxl*-97 (Sheldrick 2008). Scattering curves from neutral atoms were taken from the International Tables for Crystallography (Wilson 1992). The

Always consult and cite the final, published document. See http:/www.minsocam.org or GeoscienceWorld

occupancies of the three cation and four anion sites were initially refined using the following scattering curves: Ca at the *M*1 and *M*2 sites; As at the *T* site; O at the O1, O2, O3 sites; and F at the *X* site. Owing to the different nature of the anion species at the latter site with respect to johnbaumite, its position was found through difference-Fourier map and located at (0, 0, ¼). After a few cycles of isotropic refinement R_1 converged to 0.071, confirming the correctness of the structural model. The relatively low value of the displacement parameter at the *M*2 site suggested the partial replacement of Ca by an heavier element, i.e. Pb. Consequently, the site occupancy at the *M*2 site was refined, improving the refinement to R_1 = 0.056. After the introduction of the anisotropic displacement parameters for cations, the R_1 converged to 0.049. Assuming an anisotropic model also for the anions, the R_1 value converged to 0.032. However, the U^{33} value for the column anion *X* was high [0.119(7) Å^2], suggesting structural disorder and possibly masking the positions of other column anion sites partially occupied. Consequently, the displacement parameter of the *X* anion was refined isotropically; the refinement converged to R_1 = 0.037 and the highest residual peak was at 0.47 Å from the *X* site, at (0, 0, 0.19). This new anion position, named *X*b, was added; the sum of the site occupation factors (s.o.f.) of *X* and *X*b was constrained to 1 atom per formula unit (apfu) and their displacement parameters were forced to be equal. Owing to the similar scattering factors of oxygen and fluorine, these two elements were partitioned on the basis of the refined scattering at *X* and *X*b, assuming the F-to-OH ratio obtained through electron-microprobe data, i.e. 0.75:0.25. The *X* position at (0, 0, ¼) was assigned to F, whereas the *X*b position was considered as a mixed (F,OH) site. The refinement converged to R_1 = 0.0323 for 928 unique reflections with $F_o > 4\ \sigma(F_o)$ (0.0364 for all 1008 reflections). The structural formula derived from the structure refinement (SREF) of the studied crystal is $(Ca_{4.84}Pb_{0.16})(AsO_4)_3(F_{0.75}OH_{0.25})$, in fairly good agreement with the chemical data. Details of data collection and refinement are given in Table 2.

Always consult and cite the final, published document. See http:/www.minsocam.org or GeoscienceWorld

Crystal structure description

General features and cation coordination

Atomic coordinates, site occupancies, and isotropic or equivalent isotropic displacement parameters are reported in Table 3, and Table 4 gives anisotropic displacement parameters. Table 5 reports selected bond distances, and Table 6 shows the results of the bond-valence calculations. The bond-parameters given by Krivovichev (2012) are used for the pair Pb^{2+}–O, whereas for the other cation-anion pairs the bond-parameters are those proposed by Brese and O'Keeffe (1991).

The crystal structure of svabite is topologically similar to those of the other members of the apatite supergroup. It is composed by columns of face-sharing *M*1-centered polyhedra running along **c**; those polyhedra can be described as tricapped trigonal prisms. Adjacent columns are connected by TO_4 tetrahedra through corner-sharing. Whereas the *M*1 site is a virtually Ca pure site (a very small substitution of Na may occur, in agreement with electron-microprobe data), the *M*2 site is a mixed (Ca,Pb) site, in agreement with the preference of Pb to be hosted at this position (e.g. Lim et al. 2011). Average bond distances at these Ca-hosting sites are 2.586 and 2.485 Å for the *M*1 and *M*2 sites, respectively. These data can be compared with analogous distances in the phosphate analogue of svabite, fluorapatite, showing average distances at *M*1 and *M*2 of 2.554 and 2.463 Å (Hughes et al. 1989), respectively. Similarly, one can compare these distances with those reported in natural johnbaumite by Henderson et al. (2009), i.e. 2.62 and 2.45 Å, and by Biagioni and Pasero (2013), i.e. 2.586 and 2.480 Å. The *T* site is occupied by As, with negligible substitutions of S^{6+}, Si^{4+}, and P^{5+}. The average <*T*–O> distance is 1.674 Å, similar to the bond distance observed in johnbaumite from Harstigen (1.671 Å; Biagioni and Pasero 2013) and little shorter than that reported for johnbaumite from Franklin (1.70 Å) studied by Henderson et al. (2009).

The anion columns

Always consult and cite the final, published document. See http:/www.minsocam.org or GeoscienceWorld

Neglecting the low Cl content, the studied specimen of svabite can be defined as a member in the binary series between the endmember compositions of johnbaumite, ideally $Ca_5(AsO_4)_3OH$, and svabite, $Ca_5(AsO_4)_3F$ containing about 25 mol% johnbaumite in solid solution.

As demonstrated by Hughes et al. (1989), the anion position in binary and ternary (F-OH-Cl) apatites cannot be predicted from their positions in the endmembers. The crystal structure refinement shows two anion sites in the [001] anion columns, one at (0, 0, ¼) and the other at (0, 0, 0.19). The former is located in the *M*2 triangle within the mirror plane; it was assumed that this position is occupied by fluorine. The latter is displaced 0.39 Å above or below this plane, a position similar to that of the hydroxyl group in hydroxylapatite (Hughes et al. 1989) and johnbaumite (Biagioni and Pasero 2013); taking into account the electron microprobe data, a mixed (F,OH) occupancy at this position is suggested. The occurrence of F sites displaced from the mirror plane in anion columns has been reported by other authors, e.g. in synthetic F-Cl apatite (Hughes et al. 2014).

The split sites are actually inserted to model an electron density which is continuously distributed around the mirror plane and that is constrained by the necessity of avoiding too short anion–anion distances. Taking into account the refined anion positions, the only pair to be avoided is the $X\mathrm{b}_a$ and $X\mathrm{b}_b$, where the italic subscripts *a* and *b* correspond to *above* and *below* the mirror plane; such a pair has a distance of only ca. 2.70 Å. Other pairs have anion–anion distances ranging from 3.10 (X–$X\mathrm{b}_b$) up to 3.88 Å (X–$X\mathrm{b}_a$). A third possible anion–anion distance is represented by half of the *c* periodicity, 3.49 Å.

Bond-valence sums (BVS, in valence units, v.u.) calculated for the *X* anions, reported in Table 6, show their underbonding. The sum of the BVS at the *X* and *X*b positions is 0.78 v.u.; this underbonding is probably related to the disorder in the actual position of the column anions, and agrees with the BVS calculated by Hughes et al. (1989) for F in pure fluorapatite (i.e. 0.84 v.u.).

Always consult and cite the final, published document. See http:/www.minsocam.org or GeoscienceWorld

Discussion

Triclinic *vs* hexagonal symmetry in svabite

The prototype structure of the phases belonging to the apatite supergroup is hexagonal ($P6_3/m$); however, ordering and/or distortions can reduce the symmetry. As stated above, Baikie et al. (2007), combining diffraction data and *ab initio* calculations, obtained the $P\bar{1}$ symmetry for synthetic $Ca_5(AsO_4)_3F$. The lowering of symmetry could be due to a distortion of the unit cell required when the $M1_4(TO_4)_6$ framework is expanded with respect to the $M2_6X_2$ column contents, as a consequence of the As-to-P substitution.

Being aware of such a potential reduction of symmetry for svabite, a refinement in space group $P\bar{1}$ starting from the atomic positions given by Baikie et al. (2007) was performed. The refined triclinic unit-cell parameters of svabite are a = 9.7277(5), b = 9.7276(6), c = 6.9814(4) Å, α = 90.184(3), β = 89.931(3), γ = 120.002(2)°, as compared to the unit cell of synthetic $Ca_5(AsO_4)_3F$ given by Baikie et al. (2007): a = 9.6841(5), b = 9.6906(5), c = 6.9815(3) Å, α = 90.623(3), β = 88.869(3), γ = 120.371(3)°.

The refinement converged to R_1 = 0.028 for 11695 reflections with $F_o > 4\ \sigma(F_o)$ (0.0374 for all 14179 reflections). The structural formula derived from SREF is $(Ca_{4.84}Pb_{0.16})(AsO_4)_3(F_{0.75}OH_{0.25})$. The $(Ca:Pb)_{at.}$ ratio is the same obtained for the hexagonal model. The three independent T sites have the same average bond lengths, i.e. 1.672(2), 1.671(2), and 1.672(2) Å. The same occurs for the M sites showing indistinguishable average bond distances within the experimental errors. In addition, the three mixed (Ca,Pb) sites have the same refined $(Ca:Pb)_{at.}$ ratios. Consequently there is no convincing evidence for a lowering of symmetry in the studied sample of svabite. Even if the final R_1 value is better than for the $P6_3/m$ structure (likely as a consequence of the larger degree of freedom of the triclinic refinement), the crystal structure is

Always consult and cite the final, published document. See http:/www.minsocam.org or GeoscienceWorld

actually hexagonal; as a confirmation, the Hamilton test (Hamilton 1964, 1965) indicates that the correctness of the hexagonal model can be assumed at a confidence level > 99.5%.

The metaprism twist angle φ

A parameter used for the assessment of the distortion of the apatite structure from an ideal hexagonal close packing of oxygen is the metaprism twist angle φ, defined as the angle O1–*M*1–O2 projected on (001) (White and Dong 2003; Lim et al. 2011). The transition to lower symmetry is promoted by larger twist angle values. The twist angle φ in svabite, calculated according to the formula proposed by Henderson et al. (2009), is 21.5°, similar to that found in johnbaumite (Biagioni and Pasero 2013), i.e. 21.1°. White and Dong (2003) and White et al. (2005) pointed out that the twist angle tends to decrease like the unit-cell volume and in fact the studied crystal of svabite has an unit-cell volume larger than that of johnbaumite studied by Biagioni and Pasero (2013), i.e. 572.1 $Å^3$ to be compared with 570.4 $Å^3$, notwithstanding the slightly larger size of the hydroxyl group $(OH)^-$ with respect to F^-. The svabite studied contains ca. 0.15 Pb apfu that could explain the increase of the unit-cell volume. Taking into account the crystal structures of fluorapatite and hydroxylapatite (Hughes et al. 1989), the corresponding twist angles are 23.2 and 23.1°, respectively. The values calculated for the corresponding calcium arsenate studied in this work and by Biagioni and Pasero (2013) are smaller, in agreement with the substitution of P^{5+} by the larger cation As^{5+}. On the contrary, the twist angles obtained by Lee et al. (2009) for synthetic $Ca_5(AsO_4)_3(OH)$ and Henderson et al. (2009) for johnbaumite from Franklin are close to that of the P-analogue, i.e. 23.5°. These authors did not find any evidence of deviation from an hexagonal symmetry in their samples, even if in the $Ca_5(P_{1-x}As_xO_4)_3(OH)$ series, the twist angle anomalously decreased (Lee et al. 2009); according to Lim et al. (2011) this could suggest a change of symmetry for the OH-endmember.

Infrared spectroscopy of svabite and comparison with johnbaumite from Harstigen

Always consult and cite the final, published document. See http:/www.minsocam.org or GeoscienceWorld

The recorded FTIR spectra of svabite and johnbaumite show large similarities (Fig. 1) displaying strong absorption bands related to vibrational modes in AsO_4-tetrahedra in the range 750–950 cm^{-1} and distinct absorption related to O–H stretching modes in the range 3450-3600 cm^{-1}. In detail, however, the integrated intensity of the O–H stretching bands in the spectra of svabite is merely 34% of that recorded in spectra of the johnbaumite reference crystals (Fig. 1). This observation is in good agreement with the analytical data on the johnbaumite reference material (Biagioni and Pasero 2013) and the present svabite indicating a $OH_{svabite}/OH_{johnbaumite}$ ratio of 0.25. The positions of the OH-bands are almost identical in spectra of the two minerals: 3496, 3526 and 3560 cm^{-1} in svabite spectra and at 3498, 3528 and 3559 cm^{-1} in the johnbaumite spectra. Based on the correlation between energies of O–H stretching bands and hydrogen bonds in minerals (Libowitzky 1999) the O···H distances in the two minerals are expected to be in the range 2.04–2.17 Å. Using the IR method for determining OH concentration in apatite (Wang et al. 2011), H_2O contents in the present svabite and johnbaumite samples are calculated as 0.17 and 0.50 wt%, respectively. These calculated H_2O concentrations are approximately one half that determined by structure refinement. A likely cause for this difference may be that the molar absorption coefficients ε for O–H stretching bands in spectra of the arsenates of the apatite supergroup are lower than for corresponding bands in spectra of the phosphates belonging to this supergroup. Consequently, application of calibration based on spectra of hydroxylapatite will result in underestimation of H_2O concentrations in arsenate minerals, e.g. johnbaumite and svabite. Absorption bands related to vibrational modes in AsO_4 occur at 838, 853 and 877 cm^{-1} in the svabite spectrum (Fig. 1).

Svabite at the Jakobsberg mine

Sjögren (1891) described the new mineral svabite from the Harstigen mine; one year later, the same author reported the occurrence of this mineral both at Harstigen and at the Jakobsberg mine (Sjögren 1892). As stressed by Biagioni and Pasero (2013), the chemical analyses of samples from these two localities are not homogenous, showing different F/OH ratios. Indeed, the sample from

Always consult and cite the final, published document. See http:/www.minsocam.org or GeoscienceWorld

Harstigen is OH-dominant, corresponding to johnbaumite. Only the sample from Jakobsberg is F-dominant and corresponds to svabite in its current definition (Pasero et al. 2010).

Wet chemical data given by Sjögren (1892), as well as electron-microprobe analysis reported by Welin (1968), agree with the chemistry of svabite reported in the present study. Calcium is partially replaced by Pb and by minor amounts of Mn and Na; arsenic is substituted by minor amounts of S, Si, and P. The occurrence of Na^{+}, S^{6+}, and Si^{4+} in the crystal structure of svabite can be interpreted as the result of two possible substitutions, i.e. i) $Ca^{2+} + As^{5+} \leftrightarrow Na^{+} + S^{6+}$, and ii) $2As^{5+} \leftrightarrow Si^{4+} + S^{6+}$. The former substitution could be related to the occurrence of a cesanite component in svabite whereas the latter could be related to the presence of an ellestadite component.

The Jakobsberg mine represents an exceptional locality for the study of the crystal chemistry of arsenate apatites. Indeed, five different species belonging to the apatite supergroup are reported from this mine, i.e. hedyphane, johnbaumite, mimetite, morelandite, and svabite, the two latter species having Jakobsberg as their type locality. As the occurrence of svabite at the Jakobsberg mine is in keeping with the original description of Sjögren (1891, 1892) who did not distinguish between OH-dominant and F-dominant calcium arsenate, we suggest that the type locality of svabite should be considered Jakobsberg and not Harstigen.

Implications

Calcium arsenate apatites are actively studied owing to their potential role as sequestrators and stabilizers of As from polluted waters, an environmental problem occurring in several areas, e.g. in south-eastern Asia (e.g., Charlet and Polya 2006). Therefore, an accurate knowledge of the crystal chemistry of these As-rich compounds is crucial for environment remediation (Rakovan and Pasteris 2015). Whereas several high-quality single-crystal structure refinements have been reported for calcium phosphate apatites (e.g. White et al. 2005), few data are available for the corresponding

Always consult and cite the final, published document. See http:/www.minsocam.org or GeoscienceWorld

283 As-analogues. Single-crystal X-ray diffraction studies have been performed by Wardojo and Hwu
284 (1996) on synthetic $Ca_5(AsO_4)_3Cl$ and Biagioni and Pasero (2013) on johnbaumite. The results of
285 the X-ray single-crystal study of the three natural calcium arsenate apatites were presented by Dai
286 and Harlow (1991) in a conference abstract, but to our knowledge the details of this work have not
287 been published.

288 The refinement of the crystal structure of svabite using single-crystal X-ray diffraction data
289 represents a new step in the knowledge of the crystal chemistry of calcium arsenate apatites. Svabite
290 displays the same features of the other members of the apatite group, with $P6_3/m$ symmetry. No
291 deviation from the ideal hexagonal symmetry was observed, in contrast to the findings of Baikie et
292 al. (2007).

293

294 ## Acknowledgments

295 We wish to thank M. Serracino who assisted us during electron-microprobe analysis. MP
296 acknowledges financial support from the University of Pisa (PRA_2015_0028). J. Hughes and J.
297 Rakovan acted as reviewers, helping us in improving the manuscript.

298

Always consult and cite the final, published document. See http:/www.minsocam.org or GeoscienceWorld

References

Baikie, T., Mercier, P.H.J., Elcombe, M.M., Kim, J.Y., Le Page, Y., Mitchell, L.D., and White, Y.J. (2007) Triclinic apatites. Acta Crystallographica, B63, 251-256.

Bauer, L.H., and Berman, H. (1930) Note on some Franklin minerals. American Mineralogist, 15, 340-348.

Biagioni, C., and Pasero, M. (2013) The crystal structure of johnbaumite, $Ca_5(AsO_4)_3OH$, the arsenate analogue of hydroxylapatite. American Mineralogist, 98, 1580-1584.

Brese, N.E., and O'Keeffe, M. (1991) Bond-valence parameters for anion-anion bonds in solids. Acta Crystallographica, B48, 152-154.

Bruker AXS Inc. (2004) APEX 2. Bruker Advanced X-ray Solutions, Madison, Wisconsin, USA.

Charlet, L., and Polya, D.A. (2006) Arsenic in shallow, reducing groundwaters in Southern Asia: an environmental health disaster. Elements, 2, 91-96.

Dai, Y.S., and Harlow, G.E. (1991) Structural relationships of arsenate apatites with their anion-devoid intermetallic phase Ca_5As_3. Geological Society of America Annual Meeting, Program and Abstracts, 23, A219.

Gaines, R.V., Skinner, H.C.W., Foord, E.E.Mason, B., and Rosenzweig, A. (1997) Dana's New Mineralogy. Wiley, New York, 1819 p.

Hamilton, W.C. (1964) Statistics in Physical Science. Estimation, hypothesis testing, and least squares. The Ronald Press Company, New York, 230 p.

Hamilton, W.C. (1965) Significance tests on the crystallographic *R* factor. Acta Crystallographica, 18, 502-510.

Henderson, C.M.B., Bell, A.M.T., Charnock, J.M., Knight, K.S., Wendlandt, R.F., Plant, D.A., and Harrison, W.J. (2009) Synchrotron X-ray absorption spectroscopy and X-ray powder diffraction studies of the structure of johnbaumite $[Ca_{10}(AsO_4)_6(OH,F)_2]$ and synthetic Pb-,

Always consult and cite the final, published document. See http:/www.minsocam.org or GeoscienceWorld

Sr- and Ba-arsenate apatites and some comments on the crystal chemistry of the apatite structure type in general. Mineralogical Magazine, 73, 433-455.

Hughes, J.M., Cameron, M., and Crowley, K.D. (1989) Structural variation in natural F, OH, and Cl apatites. American Mineralogist, 74, 870-876.

Hughes, J.M., Nekvasil, H., Ustunisik, G., Lindsley, D.H., Coraor, A.E., Vaughn, J., Phillips, B.L., McCubbin, F.M., and Woerner, W.R. (2014) Solid solution in the fluorapatite-chlorapatite binary system: High precision crystal structure refinements of synthetic F-Cl apatite. American Mineralogist, 99, 369-376.

Lee, Y.J., Stephens, P.W., Tang, Y., Li, W., Phillips, B.L., Parise, J.B., and Reeder, R.J. (2009) Arsenate substitution in hydroxylapatite: structural characterization of the $Ca_5(P_xAs_{1-x}O_4)_3OH$ solid solution. American Mineralogist, 94, 666-675.

Lim, S.C., Baikie, T., Pramana, S.S., Smith, R., and White, T.J. (2011) Apatite metaprism twin angle (φ) as a tool for crystallochemical diagnosis. Journal of Solid State Chemistry, 184, 2978-2986.

Krivovichev, S.V. (2012) Derivation of bond-valence parameters for some cation-oxygen pairs on the basis of empirical relationships between r_0 and b. Zeitschrift für Kristallographie, 227, 575-579.

Libowitzky, E. (1999) Correlation of O–H stretching frequencies and O–H···O hydrogen bond lengths in minerals. Monatshefte für Chemie, 130, 1047-1059.

Malinko, S.V., Rumyantsev, G.S., and Sidorenko, G.A. (1966) Svabite from contact-metasomatic deposits of Siberia and the Urals. Doklady Akademii Nauk SSSR, 166, 134-137.

Palache, C., Berman, H., and Frondel, C. (1951) The System of Mineralogy. Volume II, 7th Ed., 1124 pp., Wiley, New York.

Always consult and cite the final, published document. See http:/www.minsocam.org or GeoscienceWorld

Pasero, M., Kampf, A.R., Ferraris, C., Pekov, I.V., Rakovan, J., and White, T.J. (2010) Nomenclautre of the apatite supergroup minerals. European Journal of Mineralogy, 22, 163-179.

Pouchou, J.L., and Pichoir, F. (1991) Quantitative analysis of homogeneous or stratified microvolumes applying the model "PAP". In K.F.J. Heinrich, D.E. Newbury, Eds., Electron Probe Quantitation, p. 31-75, Plenum Press, New York.

Rakovan, J.F., and Pasteris, G.D. (2015) A Technological Gem: Materials, Medical, and Environmental Mineralogy of Apatite. Elements, 11, 195-200.

Sheldrick, G.M. (2008) A short history of SHELX. Acta Crystallographica, A64, 112-122.

Sjögren, H. (1891) Svabit, ett mineral af apatitgruppen från Harstigsgrufvan. Geologiska Föreningen i Stockholm Förhandlingar, 13, 789-796.

Sjögren, H. (1892) Contributions to Swedish mineralogy. Part I: 7. Svabite a new member of the apatite group. Bulletin of the Geological Institution of the University of Upsala, 1, 50-56.

Wang, K.L., Zhang,Y., and Naab, F.U. (2011) Calibration for IR measurements of OH in apatite. American Mineralogist, 96, 1392-1397.

Wardojo, T.A., and Hwu, S.J. (1996) Chlorapatite: $Ca_5(AsO_4)_3Cl$. Acta Crystallographica, C52, 2959-2960.

Welin, E. (1968) X-ray powder data for minerals from Långban and the related mineral deposits of Central Sweden. Arkiv för Mineralogi och Geologi, 4, 499–541.

White, T.J., and Dong, Z. (2003) Structural derivation and crystal chemistry of apatites. Acta Crystallographica, B59, 1-16.

White, T., Ferraris, C., Kim, J., and Madhavi, S. (2005) Apatite – An adaptive framework structure. In G. Ferraris, S. Merlino, Eds., Micro- and Mesoporous Mineral Phases, 57, p. 307-401, Reviews in Mineralogy and Geochemistry, Mineralogical Society of America, Chantilly, Virginia.

Always consult and cite the final, published document. See http:/www.minsocam.org or GeoscienceWorld

371 Wilson, A.J.C. (1992) International Tables for Crystallography Volume C. Kluwer, Dordrecht.

372

373

Always consult and cite the final, published document. See http:/www.minsocam.org or GeoscienceWorld

Table captions

Table 1 – Electron-microprobe data (mean of 10 spot analysis, in wt%) of svabite and atoms per formula unit (*apfu*), on the basis of 13 anions.

Table 2 – Crystal data and summary of parameters describing data collection and refinement for svabite.

Table 3 – Site occupancies, atomic coordinates, and isotropic (*) or equivalent isotropic displacement parameters (in $Å^2$) for svabite. $U_{eq/iso}$ is defined as one third of the trace of the orthogonalized U_{ij} tensor.

Table 4 – Anisotropic displacement parameters (in $Å^2$) for svabite.

Table 5 – Selected bond distances (in Å) for svabite.

Table 6 – Bond-valence calculations for svabite, in valence unit (v.u.).

Figure captions

Fig. 1 – Infrared spectra of svabite and johnbaumite from Harstigen. (a) Polarised single-crystal IR-spectra of svabite and johnbaumite; (b) polarised single-crystal IR-spectra of svabite and johnbaumite in the OH stretching region; (c) unpolarised IR-spectrum of powdered svabite in a pressed KBr disc.

Always consult and cite the final, published document. See http:/www.minsocam.org or GeoscienceWorld

391 **Table 1** – Electron-microprobe data (mean of 10 spot analysis, in wt%) of svabite and atoms per

392 formula unit (*apfu*), on the basis of 13 anions.

Oxide	wt%	range	e.s.d.
SO_3	0.49	0.41 – 0.57	0.05
As_2O_5	51.21	50.63 – 51.93	0.38
P_2O_5	0.21	0.15 – 0.25	0.03
V_2O_5	0.04	0.00 – 0.10	0.03
SiO_2	0.19	0.10 – 0.25	0.04
CaO	39.31	38.79 – 39.87	0.28
MnO	0.48	0.43 – 0.55	0.04
SrO	0.03	0.00 – 0.07	0.02
BaO	0.01	0.00 – 0.04	0.01
PbO	5.19	4.90 – 5.36	0.15
Na_2O	0.13	0.09 – 0.16	0.02
F	2.12	1.72 – 2.49	0.22
Cl	0.08	0.06 – 0.13	0.02
H_2O*	0.33	0.15 – 0.52	0.11
O = (F+Cl)	-0.91		
Total	98.90	98.28 – 100.30	0.55

Element	apfu	range	e.s.d.
S^{6+}	0.041	0.035 – 0.048	0.004
As^{5+}	2.962	2.942 – 2.981	0.010
P^{5+}	0.019	0.014 – 0.023	0.003
V^{5+}	0.003	0.000 – 0.007	0.002
Si^{4+}	0.021	0.011 – 0.027	0.004
Ca^{2+}	4.660	4.631 – 4.697	0.024
Mn^{2+}	0.045	0.040 – 0.052	0.004
Sr^{2+}	0.002	0.000 -0.005	0.002
Ba^{2+}	0.000	0.000 – 0.002	0.001
Pb^{2+}	0.155	0.146 – 0.160	0.004
Na^{+}	0.029	0.020 – 0.035	0.004
F^{-}	0.743	0.600 – 0.875	0.078
OH^{-}	0.243	0.110 – 0.383	0.079
Cl^{-}	0.014	0.010 – 0.025	0.004

393 *recalculated in order to achieve 1 (F+OH+Cl) *pfu*.

394

Table 2 – Crystal data and summary of parameters describing data collection and refinement for svabite.

Crystal data	
Structural formula	$(Ca_{4.84}Pb_{0.16})(AsO_4)_3[F_{0.75}(OH)_{0.25}]$
Crystal size (mm)	0.23 x 0.08 x 0.05
Cell setting, space group	Hexagonal, $P6_3/m$
a, c (Å)	9.7268(5), 6.9820(4)
V (Å^3)	572.07(5)
Z	2
Data collection and refinement	
Radiation, wavelength (Å)	Mo$K\alpha$, 0.71073
Temperature (K)	298
Detector-to-sample distance (mm)	50
Number of frames	3035
Rotation width per frame (°)	0.5
Maximum observed 2θ (°)	73.70
Measured reflections	14160
Unique reflections	1008
Reflections $F_o > 4\sigma(F_o)$	928
R_{int} after absorption correction	0.0539
R_σ	0.0266
Range of h, k, l	$-16 \le h \le 15$ $-16 \le k \le 15$ $-11 \le l \le 10$
R_1 [$F_o > 4\ \sigma(F_o)$]	0.0323
R_1 (all data)	0.0364
wR_2 (on F^2_o)	0.0706
Goof	1.158
Number of l.s. parameters	40
Maximum and minimum residual	1.18 (at 0.74 Å from T) -1.03 (at 1.64 Å from O1)

400 **Table 3** – Site occupancies, atomic coordinates, and isotropic (*) or equivalent isotropic

401 displacement parameters (in Å^2) for svabite. $U_{eq/iso}$ is defined as one third of the trace of the

402 orthogonalized U_{ij} tensor.

Site	Occupancy	*x*/*a*	*y*/*b*	*z*/*c*	$U_{eq/iso}$
T	$As_{1.00}$	0.39945(5)	0.37179(5)	¼	0.0100(1)
*M*1	$Ca_{1.00}$	2/3	1/3	-0.0029(2)	0.0149(2)
*M*2	$Ca_{0.95(1)}Pb_{0.05(1)}$	0.2436(1)	0.9990(1)	¼	0.0139(2)
O1	$O_{1.00}$	0.3245(4)	0.4933(4)	¼	0.0178(6)
O2	$O_{1.00}$	0.5990(4)	0.4702(4)	¼	0.0212(7)
O3	$O_{1.00}$	0.3415(4)	0.2521(3)	0.4412(4)	0.0280(6)
X	$F_{0.45}$	0	0	¼	0.0207(14)*
*X*b	$F_{0.30}(OH)_{0.25}$	0	0	0.195(2)	0.0207(14)*

403

404

405 **Table 4** – Anisotropic displacement parameters (in Å^2) for svabite.

Site	U^{11}	U^{22}	U^{33}	U^{23}	U^{13}	U^{12}
T	0.0106(2)	0.0097(2)	0.0103(2)	0	0	0.0056(2)
*M*1	0.0183(2)	0.0183(2)	0.0082(4)	0	0	0.0092(1)
*M*2	0.0158(3)	0.0140(3)	0.0118(3)	0	0	0.0074(2)
O1	0.0258(15)	0.0161(13)	0.0172(14)	0	0	0.0148(12)
O2	0.0115(12)	0.0141(13)	0.0364(20)	0	0	0.0053(10)
O3	0.0504(16)	0.0263(12)	0.0173(11)	0.0094(10)	0.0164(11)	0.0268(12)

406

407 **Table 5** – Selected bond distances (in Å) for svabite.

408

*M*1	O1 (× 3)	2.384(2)	*M*2	O3 (× 2)	2.338(3)	*T*	O1	1.670(3)
	O2 (× 3)	2.490(2)		*X*	2.374(1)		O3 (× 2)	1.673(2)
	O3 (× 3)	2.883(3)		*X*b	2.405(2)		O2	1.681(3)
				O2	2.415(3)			
				O3 (× 2)	2.531(3)			
				O1	2.853(4)			
	<*M*1-O>	2.586		<*M*2-O>	2.485		<*T*-O>	1.674

409

410

411 **Table 6** – Bond-valence calculations for svabite, in valence unit (v.u.).

Site	O1	O2	O3	*X*	*X*b	Σ cations
*M*1	$^{3x}0.32^{\times 2}$	$^{3x}0.24^{\times 2}$	$^{3x}0.08$			1.92
*M*2	0.09	0.30	$^{2x}0.37$ $^{2x}0.22$	$0.11^{\times 3}$	$0.15^{\times 3}$	1.83
T	1.30	1.26	$^{2x}1.29$			5.14
Σ anions	2.03	2.04	1.96	0.33	0.45	

Note: left and right superscripts indicates the number of equivalent bonds involving cations and anions, respectively.

412

413

414

Fig. 1 – Infrared spectra of svabite and johnbaumite from Harstigen. (a) Polarised single-crystal IR-spectra of svabite and johnbaumite; (b) polarised single-crystal IR-spectra of svabite and johnbaumite in the OH stretching region; (c) unpolarised IR-spectrum of powdered svabite in a pressed KBr disc.

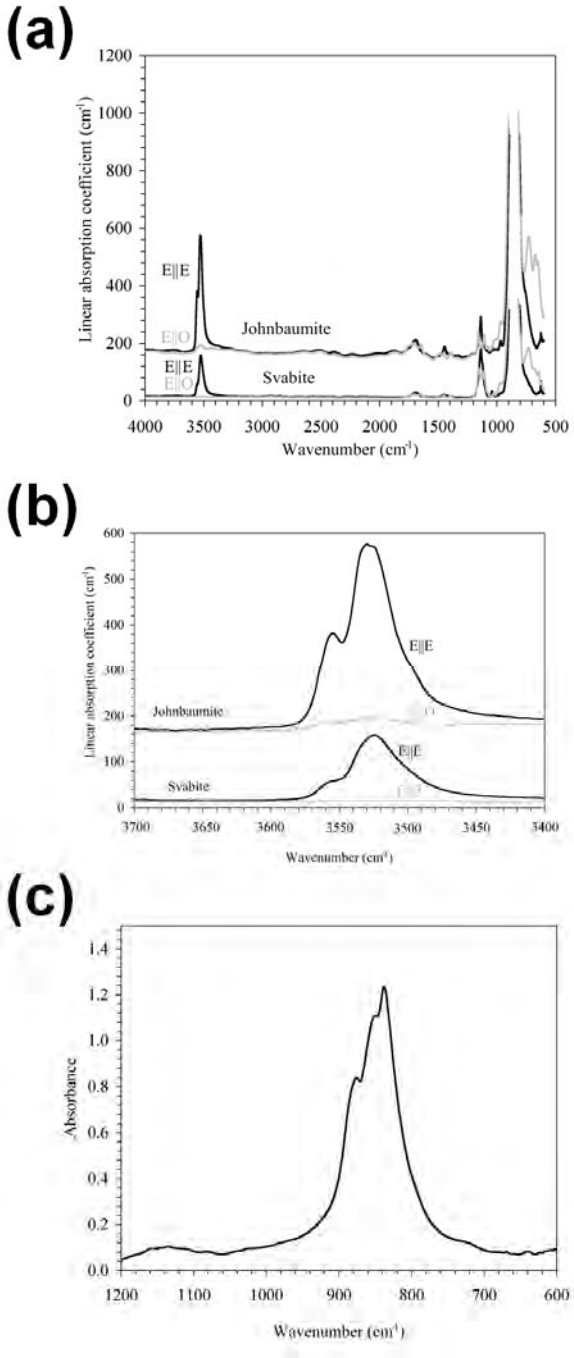

(a)

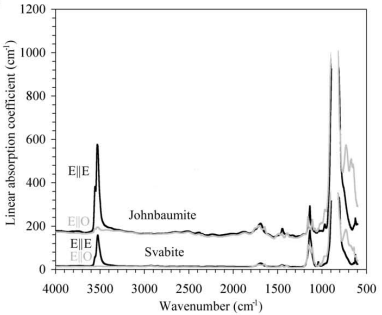
Linear absorption coefficient (cm-1)
Wavenumber (cm-1)
E||E
E⊥O
Johnbaumite
E||E
E⊥O
Svabite

(b)

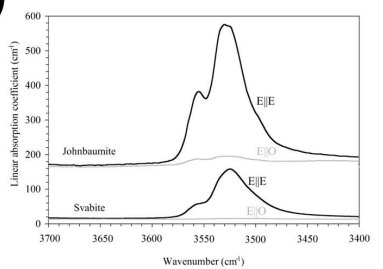
Linear absorption coefficient (cm-1)
Wavenumber (cm-1)
Johnbaumite
E||E
E⊥O
Svabite
E||E
E⊥O

(c)

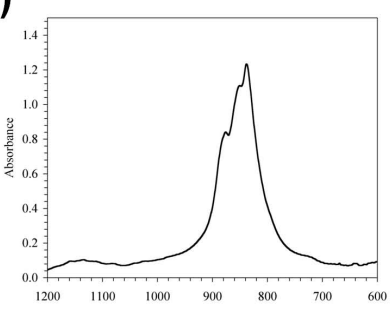
Absorbance
Wavenumber (cm-1)